

MOLECULAR DYNAMICS SIMULATION OF THERMAL CONDUCTIVITY OF NANOCRYSTALLINE COMPOSITE FILMS

N.A. Roberts, D.G. Walker* and D.Y. Li
Department of Mechanical Engineering
Vanderbilt University
Nashville, TN USA, 37235

ABSTRACT

The effectiveness of a thermoelectric device is measured by the figure of merit ZT , which is inversely proportional to the thermal conductivity. Superlattice materials often have a reduced thermal conductivity because of the introduction of interface scattering and, therefore, improved performance. The present work is focused on the effective thermal conductivity of nanocomposite films. This configuration could also improve ZT because of phonon-interface scattering introduced by the nanocrystals. The effects of crystal size and mass fraction is studied numerically using a molecular dynamics simulation. Results indicate that a reduction in the effective thermal conductivity can be achieved with the addition of a nanocrystal.

NOMENCLATURE

a lattice constant (m)
 k thermal conductivity (W/mK)
 L device length (m)
 N number of atoms
 n number fraction
 r interatomic distance (m)
 r_{cut} cutoff radius (m)
 S Seebeck coefficient ($\mu\text{V}/\text{K}$)
 T temperature (K)
 U interatomic potential (J)
 ZT thermoelectric figure of merit
 ε energy parameter (J)

σ lattice parameter (m)
 ξ crystal radius (m)

INTRODUCTION

Nanostructured materials hold great promise for high performance thermoelectric energy conversion devices. Nanocrystalline composites (NCC), which are bulk materials with embedded nanoparticles, may provide a favorable combination of effects that result in significant improvements in thermoelectric performance [1]. In particular, these materials show a decrease in thermal conductivity, which is inversely proportional the thermoelectric figure of merit (ZT). Two recent experiments [2, 3] have shown that single crystalline composite materials with embedded nanoparticles or quantum dots exhibit an increased thermoelectric figure of merit ($ZT \approx 2$). This performance is in sharp contrast to that of previous efforts that use alloys to improve thermoelectric energy conversion yielding values for ZT no larger than 1 at room temperature [4]. This dramatic improvement is, in large part, a result of the reduction in the thermal conductivity.

Measurements of thermal conductivity in superlattices have also shown a significant reduction, and the mechanisms for this reduction include interface scattering [5, 6], phonon phase interference introduced by the periodicity of the lattice [7], or phonon band creation [8]. Molecular dynamics studies by Chen et al. [9] suggest that the reduction is largely diffuse scattering at the interface for lattice mismatched materials. For lattice matched materials, phonon interference and phonon band formation dominate and a minimum occurs for a period length comparable to the dominant phonon wavelength.

*Address all correspondence to this author.

For nanocrystalline composites, the scattering mechanism is not likely a wave interference phenomenon. Instead, the scattering is particle-like because the periodicity in [3] is much larger than the phonon wavelength. The added particles, then, must be particularly efficient scatterers. Their theory is that the scattering rate is proportional to the scattering cross section, which is related to the particle size. The size dependence of the scattering in [3] supports their hypothesis. However, detailed analysis has yet to confirm this premise.

The present effort systematically studies the effect of the size of nanoparticles with molecular dynamics for phonon transport. The present work seeks to examine the thermal transport aspect of the thermoelectric performance issue in nanocomposite materials. The analysis involves a molecular dynamics study of a periodic array of crystals of varying sizes and atomic number fraction. In particular, we want to examine and explain the reduction in the thermal conductivity for NCC and understand how the structure exhibits a thermal conductivity lower than the allow limit.

ANALYSIS

In the present work, the effective thermal conductivity of a composite material is investigated using molecular dynamics [10]. The composite structure is composed of a matrix material (Ar) with embedded nanocrystals of a different material (Kr). In one set of simulations, the nanocrystal is located at the center of the wire and the radius ξ is systematically varied. In another set of simulations, half of the atoms are of one type and the other half of the other type. For this fixed number ratio, the size of the continuous regions of similar types is varied. Figure 1 shows the various structures investigated in this study.

An FCC crystalline structure is assumed with a Lennard-Jones interatomic potential given as

$$U = 4\epsilon \left[\left(\frac{\sigma}{r} \right)^{12} - \left(\frac{\sigma}{r} \right)^6 \right]. \quad (1)$$

The devices contain two materials whose property values are given in Table 1. The film is treated as a periodic lattice in the plane perpendicular to transport. In the transport direction, the device is finite.

For the simulations, a time step of 1 fs for 400,000 time steps was used where the data begins recording after 20,000 time steps to reach a quasi-steady state. The time step and length of the simulation (0.4 ns) were obtained from the thermal relaxation time of argon. The size of the device used for these simulations was $8 \times 8 \times 8$ unit cells with an additional 10 unit cells (5 on each side) in the direction of transport for the wall and bath. This configuration was used to minimize the impact of the boundaries on the thermal conductivity which has been verified by Lukes [11].

Table 1. Parameters used for the different materials in the simulations [10]. For potentials between different atoms, the energy parameter $\epsilon_{12} = \sqrt{\epsilon_1 \epsilon_2}$ and the length parameter $\sigma_{12} = (\sigma_1 + \sigma_2)/2$.

Material	Parameter	Value
Kr	ϵ (J)	2.25×10^{-21}
	σ (m)	3.65×10^{-10}
	a (m)	5.69×10^{-10}
	m (kg)	1.39×10^{-25}
	r_{cut} (m)	9.49×10^{-10}
Ar	ϵ (J)	1.67×10^{-21}
	σ (m)	3.4×10^{-10}
	a (m)	5.3×10^{-10}
	m (kg)	6.63×10^{-25}
	r_{cut} (m)	8.84×10^{-10}

The entire device is composed of 4,608 atoms, 2,560 are wall and bath atoms. The bath temperatures are held constant at 40 K and 60 K for the cold and hot sides respectively, with an initial temperature of 50 K.

The effective thermal conductivity is calculated from Fourier's law for steady conduction,

$$q = -kA \frac{\Delta T}{L}, \quad (2)$$

where L is the length of the device between the two constant bath layers. Fourier's law is assumed to be valid due to the relatively constant behaviour of the heat flux through each plane within the domain. The heat transfer q is found using the non-equilibrium molecular dynamics approach outlined by Ikeshoji [12], and the temperature is found by totaling the kinetic energy in the bath. Using kinetic arguments, the temperature is found from

$$\frac{3}{2} N k_B T = \sum_i \frac{1}{2} m_i v_i^2, \quad (3)$$

N is the number of atoms in each bath. In contrast to the technique provided by Ikeshoji [12], our bath is held at a constant temperature by adjusting the energy added at each time step. As such, the temperature difference in equation 2 is fixed and the heat flux can be obtained from the running average of the amount of energy added to maintain that temperature difference. The flux is averaged over long times [11] to establish a stable value for the heat flux.

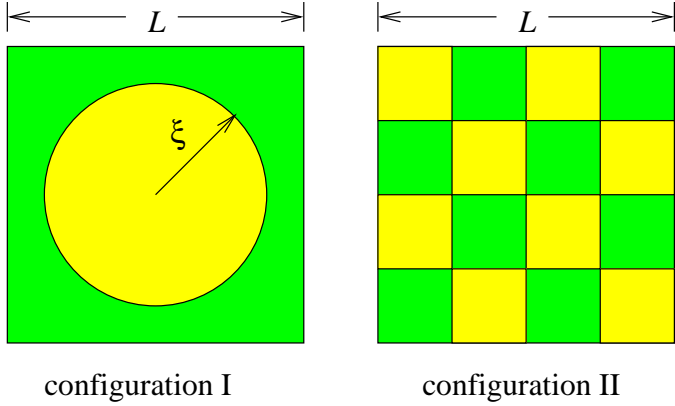


Figure 1. Two-dimensional representation of different configurations considered for effective thermal conductivity calculations. In configuration I, the radius ξ is varied. In configuration II, the period of the alternating blocks is varied, and mass fraction is held constant.

RESULTS

In the first set of analyses (configuration I in Figure 1), a crystal was placed in the center of the film and its size was varied. The crystal consists of krypton and the surrounding lattice is argon. As the radius of the crystal ξ is increased, two effects are observed. First, the krypton has a higher conductivity compared to argon, therefore as the number of krypton atoms increases, the conductivity should also increase. However, because of the lattice mismatch between the krypton and argon, an additional thermal resistance is introduced in the form of interface-phonon scattering [10]. These two effects can be summed if the thermal resistance is considered instead of the thermal conductivity. The total resistance is then written as

$$R_{\text{tot}} = R_m + R_i, \quad (4)$$

where R_m is the contribution from the bulk material properties and R_i is the contribution from the interface.

In general, the resistance due to multiple materials (R_m) materials depends on the geometry of the constituents. In the limiting cases of purely parallel and series heat transfer, the effective resistance can be significantly different. In the case of similar conductivities, however, the parallel and series models reduce to give similar results. Because the conductivity of krypton is only 10% larger than that of argon, a series model is used for its simplicity. Consequently, the material resistance from equation 4 is found by adding the contributions from each component as

$$R_m = \frac{L}{A} \left(\frac{1-n}{k_1} + \frac{n}{k_2} \right), \quad (5)$$

where n is the fraction of atoms in the material with conductivity k_2 . For crystal diameters less than the device length, the number fraction is approximately the volume of the crystal divided by the volume of the device, so n increases as the cube of the radius ξ . The length L and area A are the length and cross sectional area of the device, respectively.

The interface resistance is presumably a function of the interface area and is expressed as a jump condition

$$R_i = A_i \frac{\Delta T}{q} = \gamma A_i, \quad (6)$$

where g is the heat flux through the interface, which is the same as in equation 2. In the present case, the temperature drop ΔT across the interface is unknown. Therefore, we introduce a fitting parameter γ to account for the non-uniformity. The surface area increases as $A_i = 4\pi\xi^2$ until $\xi = L/2$, which is the radius of an inscribed sphere (crystal) in a cube (device). At this point, the area decreases through $\xi = L/\sqrt{2}$ (the midradius) until $\xi = \sqrt{3}L/2$ (the radius of the circumscribed sphere) where the entire device is composed of krypton, which is the crystal material. Realize this model assumes that interfaces parallel to the transport direction contribute to the thermal resistance equally as much as the interfaces perpendicular to the flow. Experiments at reduced scales have shown that boundary resistance plays a significant part in reducing the overall thermal conductivity of a device. This effect can dominate in devices with characteristic lengths comparable to the mean free path of phonons [13]. Although the present case does not have true boundaries parallel to the transport direction, the crystal creates a scattering interface that is conducive to this type of thermal resistance.

An estimate of the effective conductivity is found from equation 4 as

$$k_{\text{eff}} = \frac{L}{(R_m + \gamma A_i)A}. \quad (7)$$

The results of the molecular dynamics conductivity study as a function of crystal size are shown in Figure 2 with the first order model from equation 7. The fitting parameter $\gamma = 0.01 \text{ K/m}^2\text{W}$ and the normalized conductivity of krypton $k_{Kr} = 1.13$) were set to achieve the comparison. The analytic model, however, does not consider phonon interference effects and multi-dimensional transport, so perfect agreement is not expected. Nevertheless, we observe a decrease in conductivity that appears to correspond to the increase in interface area. This feature indicates that the crystal/matrix interface plays a critical role in the effective thermal conductivity of the device.

The fitting parameter $\gamma = 0.01$ was chosen to provide a good match in the region where the crystal is smaller than the device. For larger radii, the fit is not as good. This could be due to the

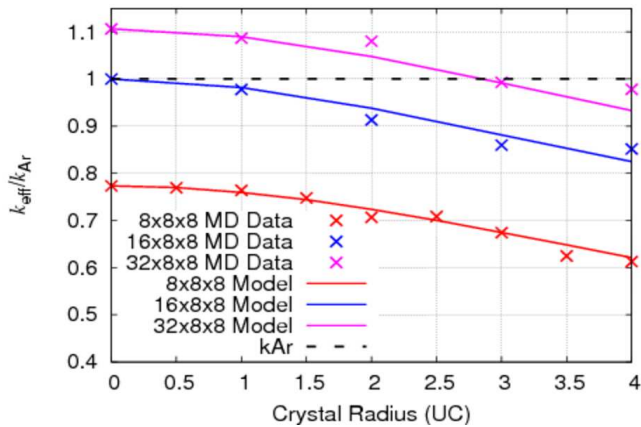


Figure 2. Dimensionless thermal conductivity as a function of the nanocrystal radius. The interface model is equation 7 for two values of γ .

fact that the bath interacts with both krypton and argon where the crystal size exceeds the device size. Consequently the bath may transfer more of its energy into the krypton and through the crystal. In this case, the bath is no longer a uniform temperature source/sink and the concept of continuum resistance as a function of area (equation 4 is no longer valid).

So far our premise is that the interface between materials results in additional scattering that decreases the effective thermal conductivity. To test this, we performed a series of simulations where the atoms were distributed randomly in the device (see Figure 3), but the fraction of krypton atoms was systematically varied. The results are shown in Figure 4. In this case, an interface area is meaningless, but we see the same characteristic decrease in the conductivity. In fact, the conductivity decreases much more. One could argue that the area of interfaces is actually quite large compared to the crystal case, and therefore, the conductivity is significantly lower. This behavior suggests that this simple system can not beat the alloy limit [3]. To investigate this premise, configuration II was used to vary the size of the crystals in the device. For this simulation the fraction of krypton atoms was held constant at 50% and the number of crystals was varied. Because our simulation domain was so small, we were limited to 3 cases. We fixed the period length of the cubic crystal to 1, 2 and 4. Figure 5 shows the results as a function of the interface area. The area available for phonon scattering is estimated as the area of a single crystal face times the number of crystals times 6 sides per crystal. By varying the crystal and placing more crystals in the domain, we can increase the area for scattering greatly. As a result we see a marked decrease in conductivity. However, these data for the highest areas are essentially the same as the randomly distributed 50% case and the conductivity is the same. Again this result suggests that we can not beat the alloy limit.

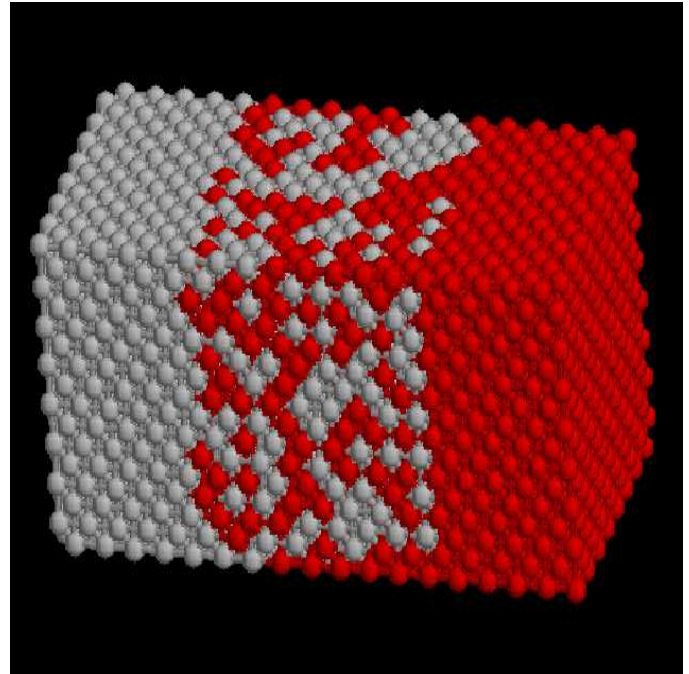


Figure 3. Example of the random distribution at 50% fraction of krypton atoms. The fraction of krypton was varied to produce the results in Figure 4.

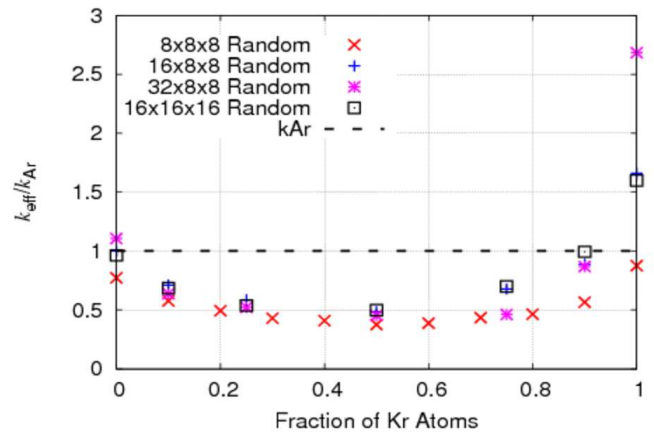


Figure 4. Dimensionless thermal conductivity as a function of the number of krypton atoms. The interface model is equation 7.

CONCLUSIONS

This paper examines the thermal conductivity of nanocrystalline composite films using the molecular dynamics computational technique. As expected, a reduced effective thermal conductivity was achieved with an increased interfacial area introduced by the nanocrystal. It was also found that the alloy limit

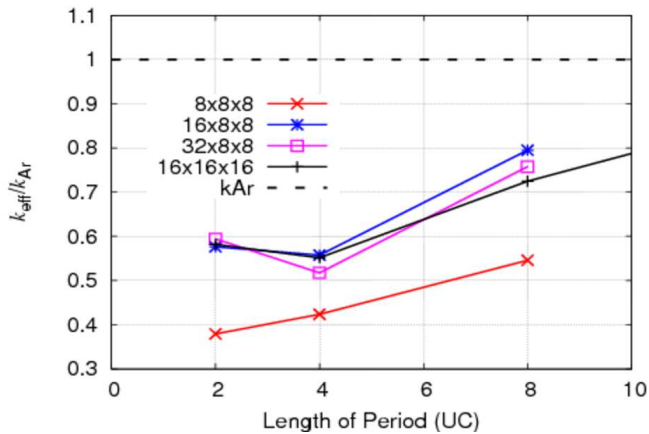


Figure 5. Dimensionless thermal conductivity as a function of interfacial area for a crystal of varying size (configuration I in Figure 1) and a fixed atomic fraction (configuration II in Figure 1).

could not be beat as determined in the comparison of the random crystal and constant atomic fraction of krypton simulations where the minimized effective thermal conductivity was approximately 50% of the solid argon film conductivity. Further work should be done to investigate the difference between interfacial effects parallel versus perpendicular to the transport direction. This work should consider confinement effects introduced by both directions.

REFERENCES

- [1] Ni, H. L., Zhao, X. B., Zhu, T. J., Ji, X. H., and Tu, J. P., 2005. "Synthesis and thermoelectric properties of Bi_2Te_3 based nanocomposites". *Journal of Alloys and Compounds*, **397**(1–2), July, pp. 317–321.
- [2] Harman, T. C., Taylor, P. J., Walsh, M. P., and La Forge, B. E., 2002. "Quantum dot superlattice thermoelectric materials and devices". *Science*, **297**(27), Sept., pp. 2229–2232.
- [3] Kim, W., Zide, J., Gossard, A., Klenov, D., Stemmer, S., Shakouri, A., and Majumdar, A., 2006. "Thermal conductivity reduction and thermoelectric figure of merit increase by embedding nanoparticles in crystalline semiconductors". *Physical Review Letters*, **96**(045901), Feb.
- [4] Service, R. F., 2006. "Semiconductor advance may help reclaim energy from 'lost' heat". *Science*, **311**(5769), Mar., pp. 1860–1860.
- [5] Capinski, W. S., Maris, H. J., Ruf, T., Cardona, M., Ploog, K., and Katzer, D. S., 1999. "Thermal-conductivity measurements of GaAs/AlAs superlattices using a picosecond optical pump-and-probe technique". *Physical Review B*, **59**(12), Mar., pp. 8105–8113.
- [6] Huxtable, S. T., Abramson, A. R., Tien, C.-L., Majumdar, A., LaBounty, C., Fan, X., Zeng, G., Bowers, J. E., Shakouri, A., and Croke, E. T., 2002. "Thermal conductivity of Si/SiGe and SiGe/SiGe superlattices". *Applied Physics Letters*, **80**(10), Mar., pp. 1737–1739.
- [7] Venkatasubramanian, R., 2000. "Lattice thermal conductivity reduction and phonon localizationlike behavior in superlattice structures". *Physical Review B*, **61**(4), Jan., pp. 3091–3097.
- [8] Simkin, M. V., and Mahan, G. D., 2000. "Minimum thermal conductivity of superlattices". *Physical review Letters*, **84**(5), January, pp. 927–930.
- [9] Chen, Y., Li, D., Lukes, J. R., Ni, Z., and Chen, M., 2005. "Minimum superlattice thermal conductivity from molecular dynamics". *Physical Review B*, **72**(174302), Nov., pp. 1–6.
- [10] Chen, Y. F., Li, D. Y., Yang, J. K., Yu, Y. H., Lukes, J. R., and Majumdar, A., 2004. "Molecular dynamics study of the lattice thermal conductivity of Kr/Ar superlattice nanowires". *Physica B—Condensed Matter*, **349**(1–4), June, pp. 270–280.
- [11] Lukes, J. R., Li, D., Liang, X.-G., and Tien, C.-L., 2000. "Molecular dynamics study of solid thin-film thermal conductivity". *Journal of Heat Transfer*, **122**(3), Aug., pp. 536–543.
- [12] Ikeshoji, T., and Hafskjold, B., 1994. "Non-equilibrium molecular dynamics calculation of heat conduction in liquid and liquid-gas interface". *Molecular Physics*, **81**(2), pp. 251–261.
- [13] Li, D. Y., Wu, Y., Fan, R., Yang, P. D., and Majumdar, A., 2003. "Thermal conductivity of Si/SiGe superlattice nanowires". *Applied Physics Letters*, **83**(15), Oct., pp. 3186–3188.